CHAPTER 6

COMBINED MODELS

6.1 PRINCIPLE OF SUPERIMPOSING DATA

The objective of this method of analysis and design is to represent both the rockmass demand and stope support capacity on a common two-dimensional graph. Both the stope support and the rockmass models described in Chapters 4 and 5 are combined and compared during the third stage of the study.

The effect that changes in some of the variables might have on the stability of the excavation is presented on the graph and its effect determined from a stability analysis of the rockmass/support interaction. This is achieved through the analysis that is described in this chapter.

Stope support element performance, or the capacity of stope support elements for timber and lightweight cementitious and timber elongates respectively are described by the combined mathematical functions given in Chapter 4 while the rockmass demand is described in terms of rockmass stiffness in Chapter 5.

The function of the support element(s) is multiplied by a factor n to compensate for the total attributed area supported by what can be a combination of different support types:

$$F(x) = \sum_{i=1}^{n} n_i . f_a(x) \quad (6.1)$$

where:

n_i = Number of support elements of say type i;
 = $A_a/(d_i.s_i)$ for the specific support type i;
A_a = Attributed area (m^2);
d_i = Dip spacing of support element type i, (m); and
s_i = Strike spacing of support element type i, (m).

This principle of superimposed data is graphically illustrated in Figure 6.1.

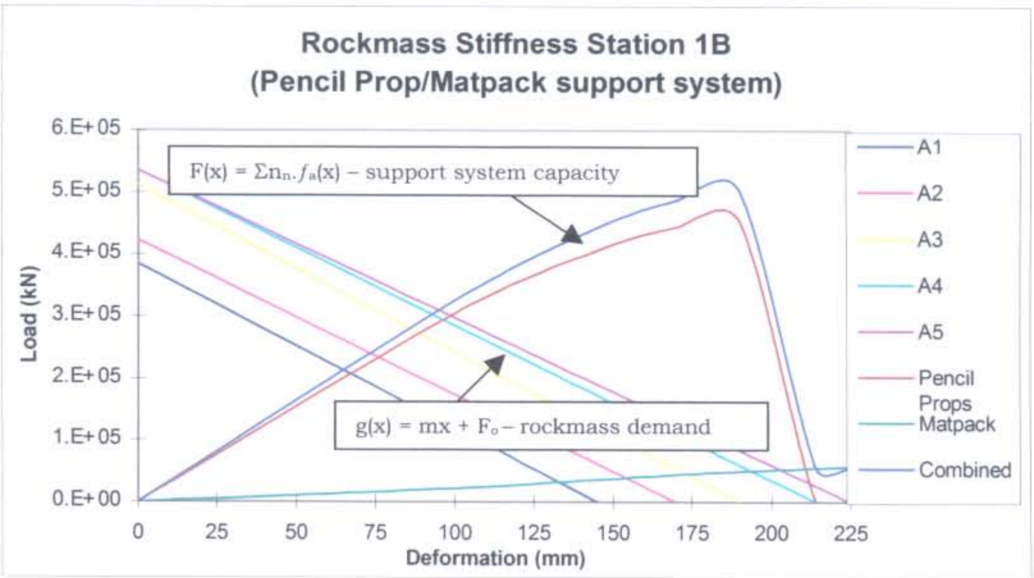

Figure 6.1: Example of graphical representation of both the rockmass and stope support models on a common force-deformation axis for 5 consecutive mining steps

Figure 6.1 shows the combined load generated by the Pencil Props and Matpacks for the given attributed area A_a. The "Combined" curve represents the sum of the forces generated by the support system as given by equation 6.1.

The load lines for the rockmass are also shown for the five consecutive mining steps A1 to A5.

6.2 STABILITY TEST

Potential instability or unstable failure will occur where the energy released by the rockmass for a given interval of deformation is more than the energy that can be absorbed or tolerated by the support system.

The following criterion is used to test for stability for any given mining geometry and/or support type:

6.2.1 Stiffness comparison

Failure of the supports occurs when the load on the support exceeds its strength. This failure may occur in a stable or unstable manner. The slopes of the lines are relevant to the post failure of the support in defining the mode of failure of the supports. Unstable failure of the support will take place when the slope of the rockmass stiffness is less than that of the post failure stiffness of that of the stope support element. Mathematically this is where:

$|m| < |F'(x)|$ as illustrated in Figure 6.2 that is where $|\tan\gamma| > |\tan\lambda|$ with angles γ and λ as shown.

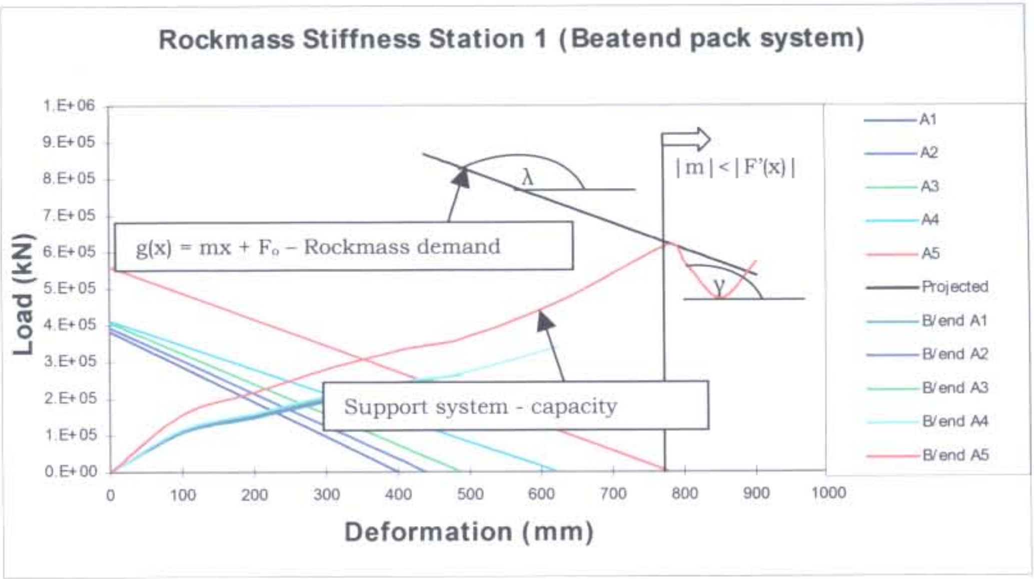

Figure 6.2: Combined models demonstrating the unstable failure of the stope support starting at 790 mm deformation during the mining stage A5

6.2.2 Energy comparison

The condition where the energy released by the rockmass for further deformation exceeds that which can be absorbed by the support will result in a potentially stable or unstable failure of the supports. The terms stable and unstable failure are defined in Chapter 9 – Glossary of terms.

Mathematically this is the true where:

$\int_a^b g(x)\partial x > \int_a^b F(x)\partial x$ for a given deformation interval. This condition will result in the unstable failure of the supports. The energy released by the rockmass and that absorbed by the stope support for the deformation interval from 780 mm to 885 mm for the last mining step A5 given in Figure 6.2 is illustrated in Figure 6.3.

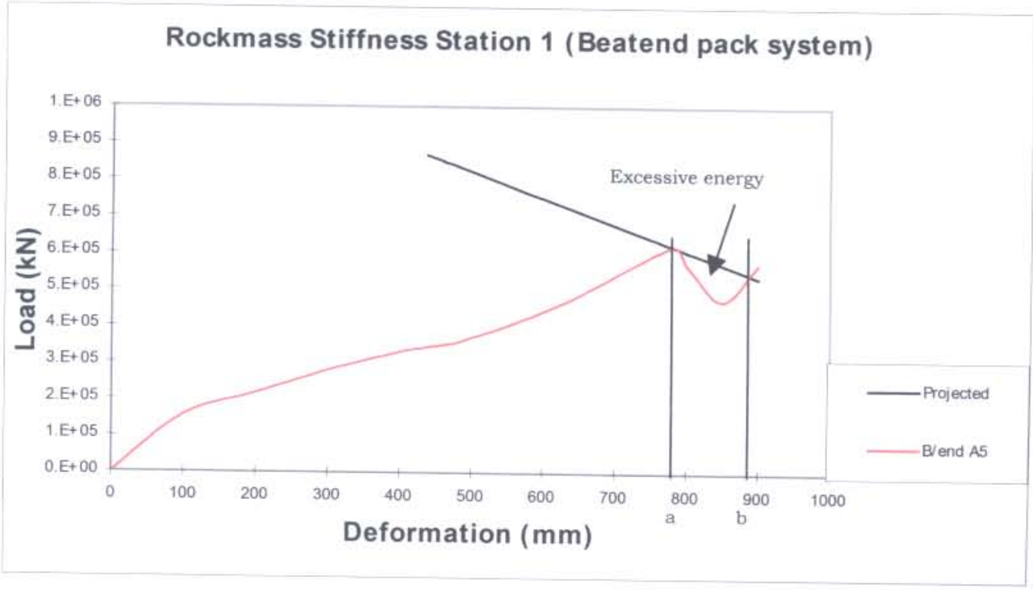

Figure 6.3: The excessive energy released by the rockmass for the given deformation interval shown by the shaded area

6.3 INPUTS AND ITS INFLUENCE ON THE COMBINED MODEL

The design process is executed on a comparative basis where different stope support and mine layout options can be compared to one another and inputs varied to examine for stability. A number of parameters have an influence on the excavation stability. The influence of each of these parameters must be evaluated in order to assess the underground layout and support combination for the purpose of a stability analysis. Each of these parameters for the rockmass and stope support system is discussed under the headings 6.3.1(a) to (g) and 6.3.2 (a) to (f). This is achieved by changing the relevant input variables and by examining the impact that it has on stability. It is through this analysis that the effect of each of those can be compared to other options and/or density of support.

6.3.1 Demand - Rockmass model

(a) Layout and configuration of underground mining environment

The rockmass stiffness is directly related to the attributed area constructed in and for the given underground excavation layout. The attributed area is constructed according to the Guidelines described in Chapter 5.

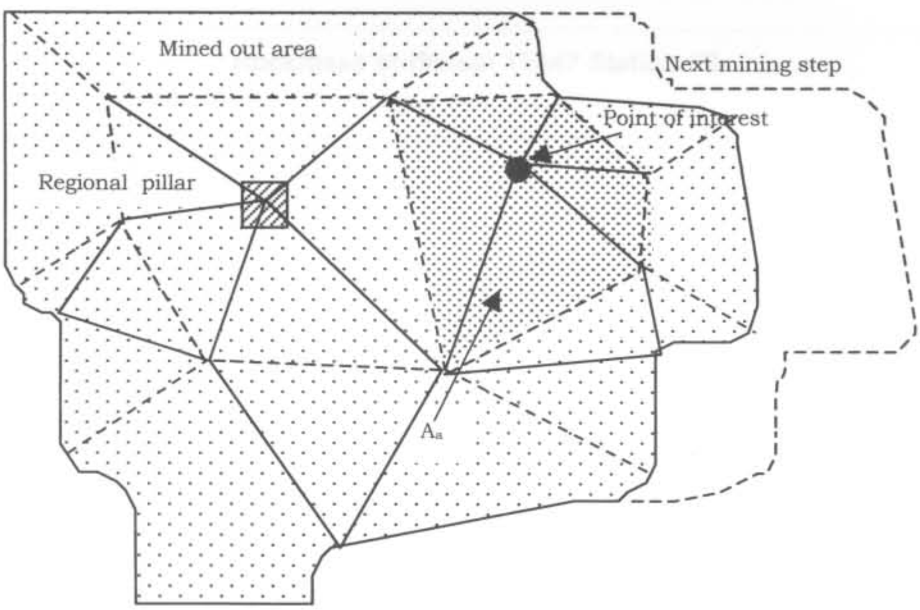

Figure 6.4: Attributed area (A_a) at the point of interest for a given mining geometry

The attributed area is influenced by the mining span and presence and position of regional support and changes in time with consecutive mining steps as illustrated in Figure 6.4. The attributed area in turn influences rockmass stiffness. The rockmass stiffness is described mathematically by the function $g(x) = mx + F_o$, with the symbols as defined previously.

The magnitude of the force F_o is a function of the attributed area, the thickness of the hangingwall beam, rockmass density and gravitational acceleration.

The rockmass stiffness is associated with the amount of closure at the point of interest. The closure at a given point in the stope is again directly related to the mining span and its proximity to the abutment and/or regional support. The mining span and presence and position of regional support therefore have a direct influence on the rockmass stiffness. The larger the amounts of deformation at any given point for the same magnitude attributed area force F_o the softer the rockmass, that is an increase in the magnitude of the angle λ as defined before.

The decrease of rockmass stiffness for consecutive mining steps (A2 to A5) and hence an increased mining span for one of the measuring stations of the 15A47 Stope is shown in Figure 6.5.

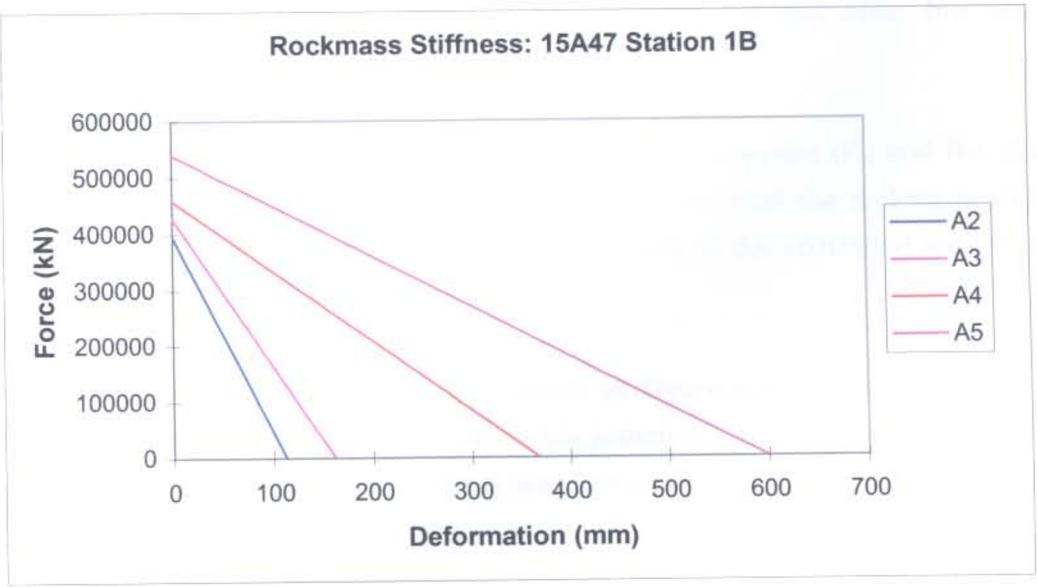

Figure 6.5: Decrease in rockmass stiffness (softening) for four consecutive mining steps

(b) Stope face position for successive mining intervals

The mining span increases as the position of the stope face is advanced. The position of the stope face relative to the point of interest (station) thus dictates the attributed area A_a as demonstrated in Figure 6.4. The further the face is away from a measuring station, the larger the mining span and hence the softer the rockmass.

(c) Position and presence of regional support

The presence and relative position of regional support influences the attributed area A_a, as demonstrated in Figure 6.4. Regional support breaks the mining span provided that the pillars remain intact. The mining span on the other hand is directly related to the attributed area A_a. The presence and position of regional support therefore has a direct influence on the rockmass stiffness since the latter is related to the mining span.

(d) Physical position of the point of interest in the stope

The attributed area is calculated for a point of interest with that point as the focal point of the attributed area calculation as demonstrated earlier. As the position of the point of interest is moved, the distances to the abutments will also change. These distances not only have a direct bearing on the shape of the attributed area, but also its attributed area (A_a).

The rockmass stiffness is determined by both the force component (F_o) and the closure measured at the particular point. From this it is apparent that the rockmass stiffness will vary from one position in the stope to the next as both the attributed area (A_a) and stope closure (deformation component) will vary.

A simple two-dimensional mining slot presented in Figure 6.6 shows that the closure varies from one point to the next illustrates this principle. The principle applies to the three dimensional models where closure was measured during the instrumentation program.

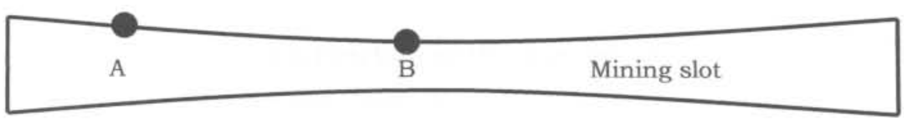

Figure 6.6: Two-dimensional mining slot showing different closure at different positions

(e) Closure at the point of interest for the different mining intervals

The rockmass stiffness is calculated from the force component (F_o) and the closure at the point of interest for a particular mining geometry. For the same magnitude force but with different closure components will the rockmass stiffness changes accordingly. The larger the stope closure (deformation) component for the same force component (F_o) the softer the rockmass i.e. the larger the angle λ, and vice versa. The closure at a given point will change with every consecutive mining interval, and hence influence rockmass stiffness.

The rockmass stiffness is therefore constantly changing at different points in the stope as mining continues. This is illustrated in Figure 6.7 where the bold printed line shows the rockmass stiffness history for measuring Station 1B during the 4 stages of mining.

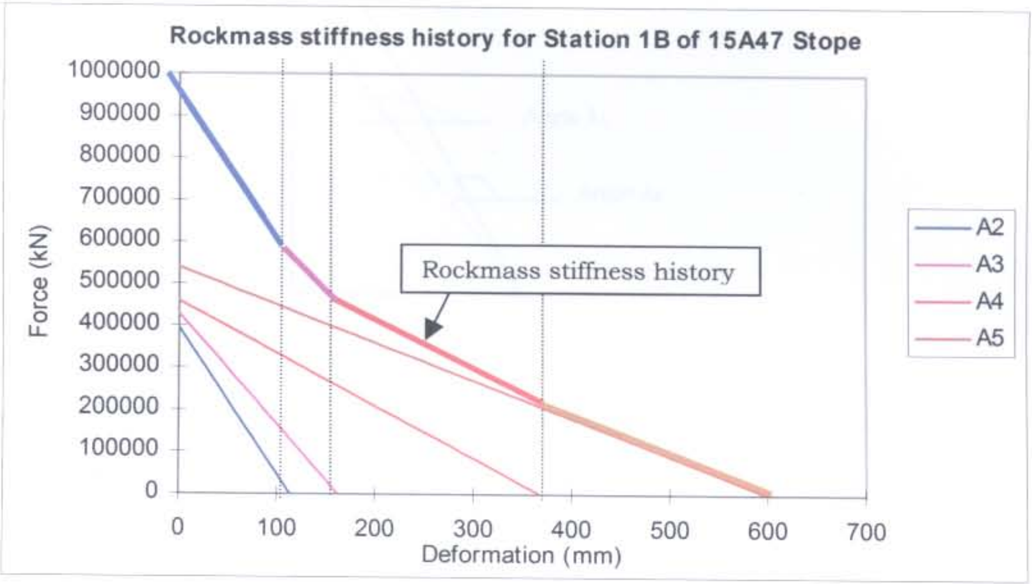

Figure 6.7: Rockmass stiffness history for a measuring station during 4 mining stages

(f) Hangingwall beam thickness

The attributed area force is (F_o) a function of the hangingwall beam thickness (m). The higher the beam thickness for the same attributed area A_a, the higher the attributed force (shown as $F_o(2)$ in Figure 6.8) will be. For the same amount of stope closure the rockmass will therefore be stiffer with an increased beam thickness. In the latter case the angle λ_2 will be smaller.

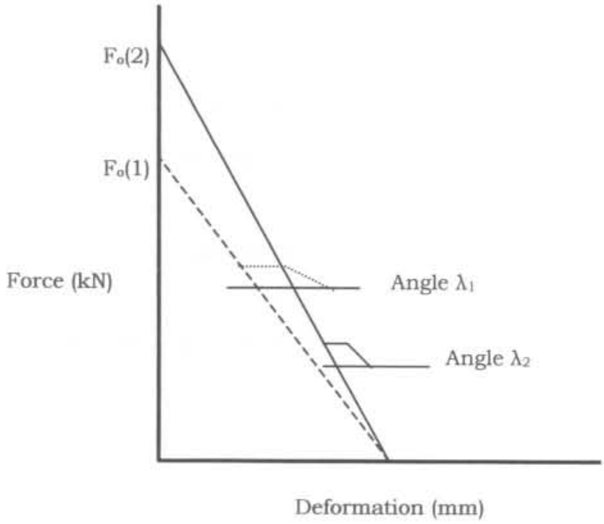

Figure 6.8(a): Effect of increased beam thickness on the rockmass stiffness with same deflection on rockmass stiffness

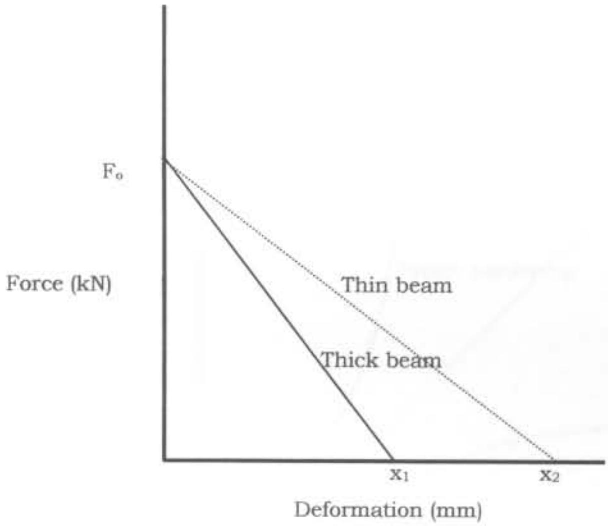

Figure 6.8(b): Effect of increased beam thickness on the rockmass stiffness with same attributed area force F_o

This principle is confirmed by the beam theory where the deflection of a beam is given as:

$$\eta \propto \gamma L^4/Et^2 \qquad (6.2)$$

with:

η = Deflection of beam (m);

γ = Weight per unit length (=ρg) (N/m);
L = Beam span (m);
E = Young's modulus of the beam material (GPa);
T = Beam thickness (m), and

where a number of thin beams will deflect more than fewer thicker ones.

6.3.2 Capacity - Stope support model

Different types of support have different performance characteristics. The support performance represents the capacity of a unit to generate load during increased deformation of the element.

The performance characteristic of a support unit is described in Chapter 4 and demonstrates the unique capacity of each of the different supports. Strain hardening refers to the situation where the load that is generated as deformation takes place increases at a non-linear rate. Strain softening refers to the condition where the load deceases non-linearly as deformation takes place.

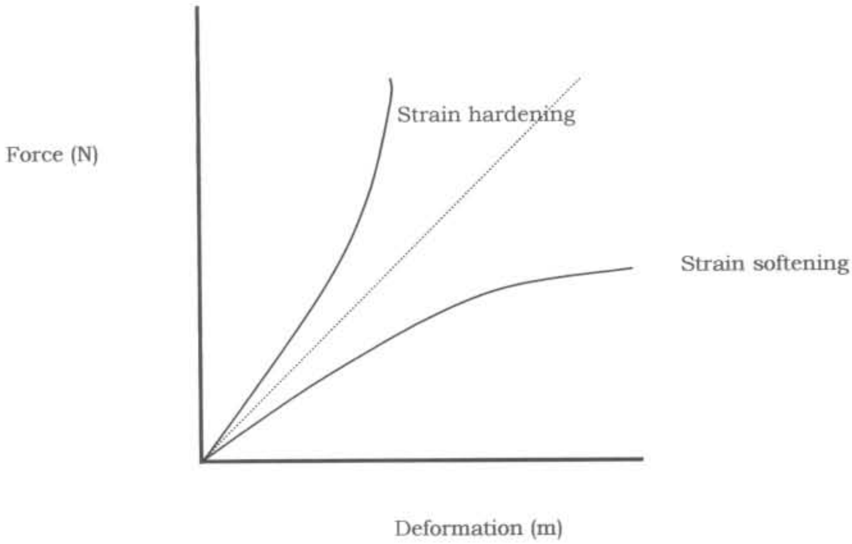

Figure 6.9 Illustration of strain hardening and strain softening of supports

Not only is the load bearing characteristics different for the various support types as deformation increases, but other factors such as loading rate and the slenderness ratio will influence its behaviour in different ways. The following aspects all form part of input to the models.

(a) Rate of deformation

The extent to which the laboratory support performance data must be up- or downgraded as a result of the effect of the rate of deformation, is a function of material type and the differences between laboratory - and underground rates of deformation and is described in detail in Chapter 4

(b) Height of pack tested versus installed

The stope width is often different to the height of the support unit that was tested. To quantify the support performance of any type of pack it is important that this is quantified and the effect that it has on the performance of such a unit taken into consideration during the design process.

(c) Buckling failure of timber elongate support

Buckling failure of an elongate has a major impact on the design of support since it dictates the stability of the unit once a certain amount of deformation is exceeded. It does not only affect the ability to absorb energy but also its stiffness. Props with an increased yield range have a higher energy absorption capacity.

Buckling failure reduces the effective yield life of an elongate and will therefore affect its capacity to absorb energy. According to Roberts (1991) high closure prior to the event reduces the ability of a yielding timber elongate to absorb energy during a rockburst.

(d) Installation spacing of support

The function of the supports is multiplied by a factor n to compensate for the number of support elements of different types that are installed to support the attributed area. This total force is calculated as:

$$F(x) = \Sigma n_n . f_a(x) \qquad (6.3)$$

where:

n_n = Number of support elements of type n;

= $A_a/(d.s)$ for the specific support type;

A_a = Attributed area (m^2);

d = Dip spacing of support elements (m); and

s = Strike spacing of support elements (m).

This principle is graphically illustrated by Figure 6.10 where the number of support elements for the given attributed area A_a is determined for a given dip and strike spacing of the specific support type.

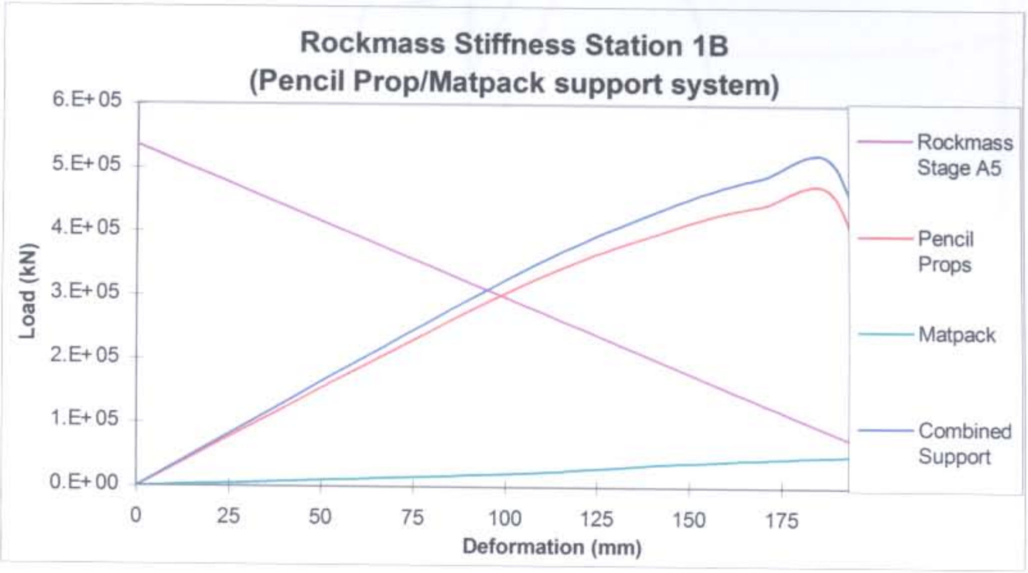

Figure 6.10: Graphical representation of rockmass and stope support models for mining stage A5

(e) Support pre-stressing

The pre-stressing of support during installation has become a routine practice in the South African mining industry. The benefit of pre stressing is the fact that the support is not blasted out that easily, and that it alters the support characteristic from passive to active. (See definition in Chapter 9: Glossary of Terms.) Both packs and elongate types of support can be pre-stressed.

Not only does the pre-stressing of a support element increase the load generated by the element upon installation but also the energy generated during the early stages of deformation since the latter relates to the area underneath the force-deformation curve.

The influence that pre-stressing of support has on its performance is illustrated in Figure 6.11 showing a 160 mm diameter Profile Prop, 1.0 m high that is pre-stressed with effective pre-stress of 100 kN. It shows the loss in pre-stress load from 100 kN to an effective 68 kN due to the creep of timber.

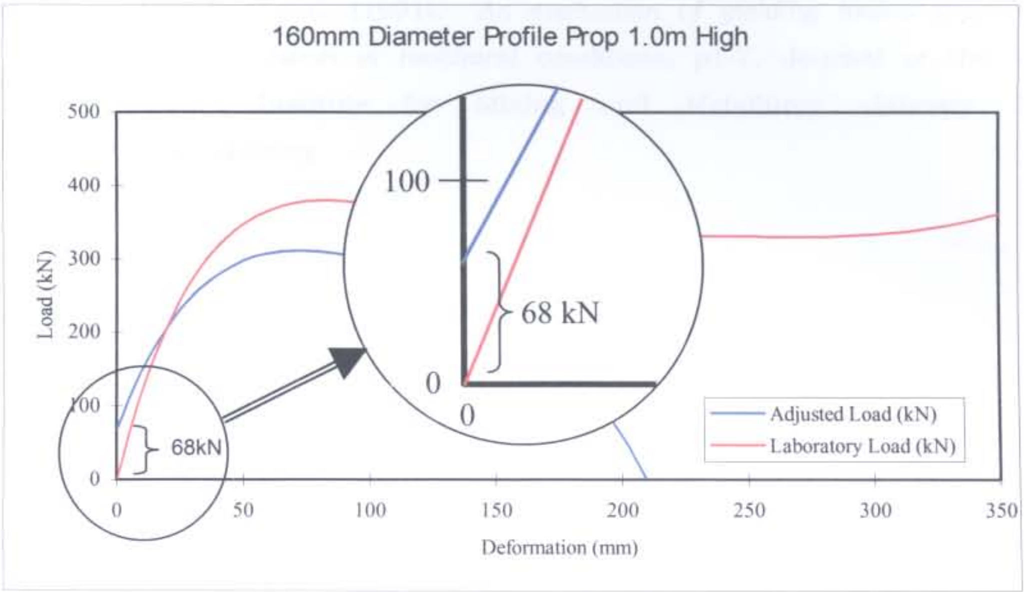

Figure 6.11: Effect of timber creep on the performance of a 160mm diameter Profile Prop

6.4 CONCLUSION

It has been demonstrated in this chapter how both the rockmass demand as well as the support capacity can be represented on a common two-dimensional force-deformation graph. Once this is achieved can a stability analysis be done where both the stiffness and the energy of the two components can be compared for a given deformation and for a given deformation interval respectively.

The inputs and its influence on to the combined model are described, and is repeated for both the rockmass as well as the stope support models.

REFERENCES

Kotze T.J. (1991). Internal rock engineering report for Beatrix Gold Mine, Gengold, South Africa.

Roberts M.K.C. (1991). *An evaluation of yielding timber props as a support system in rockburst conditions*, p1-7, Journal of the South African Institute for Mining and Metallurgy, January 1991, Johannesburg.